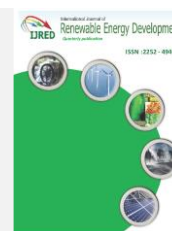




Contents list available at IJRED website

International Journal of Renewable Energy Development

Journal homepage: <https://ijred.undip.ac.id>



Research Article

# Effect of Different Hydrothermal Temperatures on the Properties on Nano-Silica (SiO<sub>2</sub>) of Rice Husk

Irzaman<sup>a\*</sup>, Irmansyah<sup>a</sup>, Siti Aisyah<sup>a</sup>, Nazopatul Patonah Har<sup>a</sup>, Aminullah<sup>b</sup>

<sup>a</sup>Department of Physics, Faculty of Mathematics and Natural Sciences, IPB University, Bogor, 16680, Indonesia

<sup>b</sup>Department of Food Technology and Nutrition, Faculty of Halal Food Science, Djuanda University, Bogor, 16720, Indonesia

**Abstract.** Rice husk has high silica (SiO<sub>2</sub>) content and can be used as the primary material for making nano-silica. One of the methods for synthesizing nano-silica was the hydrothermal method. The objective of this study was to synthesize nano-silica from rice husks by observing the effect of temperature in the hydrothermal process on the structure, electrical and particle properties of nano-silica. The hydrothermal process temperature was 150, 200, and 250 °C for 4 hours. The results showed that all nano-silicas were in the amorphous phase. The particle size was in the range of 0.16-13.49 nm with more uniform size distribution on nano-silicas of 200 °C and 250 °C than nano-silica at 150 °C. These three nano-silicas were included in the semiconductor category by increasing temperature and frequency. In addition, these treatment variations resulted 200 °C for 4 hours and pressure of 2 atm as the optimum treatment for manufacturing nano-silica of rice husk ash. This nano-silica could be used as semiconductor material for electronic industry.

**Keywords:** Amorphous; hydrothermal; semiconductor; rice husk; nano-silica size



@ The author(s). Published by CBIORE. This is an open access article under the CC BY-SA license (<http://creativecommons.org/licenses/by-sa/4.0/>)

Received: 4<sup>th</sup> Jan 2022; Revised: 15<sup>th</sup> March 2022; Accepted: 6<sup>th</sup> April 2022; Available online: 18<sup>th</sup> April 20

## 1. Introduction

Indonesia is a country with abundant natural resources potential. These potentials include oil, gas, and mineral materials. Among mineral materials, some materials are classified as oxides that have the potential to use high-tech applications such as ZnO, SiO<sub>2</sub>, MgO, Al<sub>2</sub>O<sub>3</sub>, and TiO<sub>2</sub>. Oxide materials, mainly silica, have been widely used in various applications. The most regular and commercial use of silica is the primary material for the glass industry and raw material for making solar cells (Burkowicz *et al.*, 2020; Husain *et al.*, 2018). Several studies have shown that natural-based silicas such as silica from bamboo leaf (Aminullah *et al.*, 2018; Irzaman *et al.*, 2018), baggase (Adli *et al.*, 2018), cogon grass (Irzaman *et al.*, 2021), and rice husk (Irzaman *et al.*, 2020; Rohaeti *et al.*, 2010) have been successfully purified and synthesized into silica nanoparticles. Nano-silica is used in science and industrial applications such as catalysts, pigments, pharmaceuticals, drugs, cosmetics, and food (Nabeshi *et al.*, 2011). This is because silica (SiO<sub>2</sub>) nanoparticles have good stability, are chemically inert, are biocompatible, and can work in harmony with the body's work system and form a single spherical (Yuan *et al.*, 2010). According to Khan *et al.*, (2019), nanoparticle materials are considered more efficient to use because they are defined as materials with a size of about 1-100 nm so that their surface area is larger

and undergoes specific changes compared to larger-sized materials.

According to the BPS (2019), the total rice production in Indonesia in 2019 was around 54.60 million tons of dry milled grain (DMG). Rice husk, as an abundant waste, especially in agrarian countries, is one of the largest sources of silica production. Rice husk contains silica as much as 85%-95% dry weight after complete combustion (Hossain *et al.*, 2018). However, rice husk is considered a less helpful material and has low nutritional value because rice husk has a reasonably high ash content (Deviani *et al.*, 2018). With the silica content in rice husks, this waste can be used not to cause environmental pollution by extracting silica from the rice husks so that organic silica can be used as an alternative.

Several methods are used to synthesize nano-silica, such as sol-gel, coprecipitation, polymeric gel, and hydrothermal (Hasri *et al.*, 2020; Jal *et al.*, 2004; Rahman and Padevettan, 2012; Yazdani *et al.*, 2010). Among these methods, the hydrothermal method has several advantages: it does not require high costs and has easy steps in the manufacture of nanoparticle materials. There are 3 methods in hydrothermal processing for manufacturing nanoparticles, namely temperature-difference method, temperature-reduction technique, and metastable-phase technique (Byrappa and Masahiro, 2001). This research using temperature-difference method in hydrothermal processing in manufacturing nano-silica

\* Corresponding author  
Email: [irzaman@apps.ipb.ac.id](mailto:irzaman@apps.ipb.ac.id) (Irzaman)

from rice husk ash. Yazdani *et al.* (2010) reported that nano-silica synthesis with different pressures (3, 5, and 7 atm) at 200 °C. In another previous study, Iftitahyah *et al.*, (2018) synthesized NaX zeolite from Bangka Belitung kaolin and produced the best results in 4 hours. Then Rahma (2017) synthesized sodium hexatitanate within 24 hours and produced the best results at a temperature of 150 °C. Based on these literatures, the research will synthesize nano-silica using the hydrothermal method with temperature variations of 150 °C, 200 °C and 250 °C for 4 hours and pressure of 2 atm. This study aims to determine the effect of temperature in the hydrothermal process on nano-silica from rice husks on size characteristics, size distribution (particle size analysis), crystal structure, and electrical properties.

## 2. Materials and Methods

### 2.1 Materials and Tools

The materials used in this study were dry rice husk charcoal (Hippo Grow Indonesia, Ltd., South Tangerang, Banten Province, Indonesia), 3% HCl (technical, Sigma Aldrich), 2.5 N NaOH (Merck/technical, Sigma Aldrich), 5 N H<sub>2</sub>SO<sub>4</sub> (Merck/p.a, Sigma Aldrich), and distilled water. The equipment used in this research included Particle Size Analyzer (PSA) type NanoQ, X-Rays Diffraction (XRD) type SHIMADZU XRD 7000 X-RAY MAXima Diffractometer, LCR meter type Hioki HiTESTER 3522-50, hydrothermal reactor type Parr 4848, furnace (Nabertherm GmbH), analytical balance, magnetic stirrer, and universal pH indicator.

### 2.2 Nano-silica Synthesis Process

#### 2.2.1 Preparation of Rice Husk Ash

Rice husk charcoal was weighed as much as 6 grams and then put into a porcelain dish and then burned using a kiln to avoid any impurities while making rice husk ash. The combustion process was carried out at room temperature and then raised at 450 °C and held for 2 hours. Subsequent combustion, the temperature was raised to 900 °C with the increasing temperature rate of 1.67 °C min<sup>-1</sup>, and held for 1 hour at temperature of 900 °C (Irzaman *et al.*, 2020; Rohaeti *et al.*, 2010; Verina, 2014). Then, the temperature was lowered to room temperature.

#### 2.2.2 Nano-silica Synthesis

The nano-silica synthesis process was carried out using the hydrothermal method referring to Yuvakkumar *et al.*, (2012) and Maesaroh (2020). After the ashing process, the rice husk ash was weighed and washed using a 3% HCl solution to reduce the impurities present in the rice husk ash other than silica.

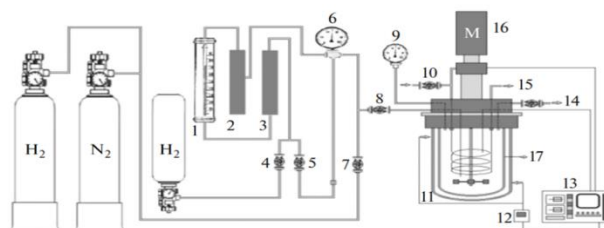


**Fig.1.** A schematic figure of the high-pressure Parr 4848 reactor system: (1) high pressure burette; (2, 3) balancing columns; (4, 5, 7) taps; (6, 9) monometers; (8) gas line; (11) electric heater; (12) valve; (13) temperature and speed controller; (14) sampling tap; (10,15) cooling line; (16) mixer (0–2000 rpm); (17) reactor. (Toshtay & Auezov, 2020).

The washing process was carried out as follows: first, rice husk ash was put into a beaker glass and mixed with 3% HCl in a ratio of 12 mL of 3% HCl for 1 gram of rice husk ash, then heated at 200 °C on a hotplate and stirred at high speed of 240 rpm using a magnetic stirrer for 2 hours. After that, the sample was filtered using filter paper, and the precipitate was taken. The precipitate was washed using warm distilled water repeatedly until it was free of acid. The acid-free precipitate was dissolved as much as 5 grams into 150 mL of 2.5 N NaOH while stirring using a magnetic stirrer at 80 °C at a speed of 240 rpm for 3.5 hours.

The sodium silicate was then put into a hydrothermal reactor with 150 °C, 200 °C, and 250 °C for 4 hours and pressure of 2 atm. A schematic diagram of hydrothermal reactor type Parr 4848 was shown in Fig. 1. The results of the hydrothermal process were then filtered using filter paper to separate them from the residue. Next, the filtration results were titrated with 5 N H<sub>2</sub>SO<sub>4</sub> while stirring using a magnetic stirrer to pH 2 to extract the nano-silica precipitate. The precipitate obtained was then filtered and washed using distilled water until the pH was neutral. The filtration results were then calcined at a temperature of 500 °C using a furnace for 3 hours (Yuvakkumar *et al.*, 2012). The final result of this calcination process was a white silica powder.

### 2.3 Nano-silica Characterization

#### 2.3.1 Structure analysis

Samples were prepared as much as 0.3 grams and then scanned by XRD XPERT-PRO starting from an angle of 5° to 90° with a Cu-Kα1 radiation source with  $\lambda = 1.5406 \text{ \AA}$ , the generator voltage is 40 kV. The average crystallite size and nano-silica lattice strain from the XRD pattern using the Scherrer equation (1).

$$\beta \cos \theta = \frac{0.9\lambda}{D} + 4\eta \sin \theta \quad (1)$$

where  $\beta$  was the maximum half-peak width (FWHM),  $D$  was the crystallite size,  $\lambda$  was the X-ray wavelength,  $\eta$  was the lattice strain and  $\theta$  was the diffraction angle. Crystal size and lattice strain were calculated using the curve between  $\beta \cos \theta$  to  $4\eta \sin \theta$  so that linear regression lines were obtained for all compositions (Nasir *et al.*, 2020).

#### 2.3.2 Particle size analysis

Samples resulting from the hydrothermal process with temperature variations of 150 °C, 200 °C, and 250 °C were characterized to observe particle size and particle distribution using PSA (Particle Size Analyzer) Nano-Q. First, the sample was prepared by dispersing 0.02 grams of nano-silica in 10 ml of distilled water. Then the solution was measured using PSA for 1-2 minutes. The particle size data obtained were in the form of three distributions, namely intensity, number, and volume, to describe the overall state of the sample (Nikmatin *et al.*, 2012).

#### 2.3.3 Electrical conductivity analysis

Samples resulting from the hydrothermal process with temperature variations of 150 °C, 200 °C, and 250 °C were characterized using an LCR meter type Hioki HiTESTER 3522-50. LCR meter was used to determine the electrical properties of a material. One of the electrical properties that were read on the LCR device was conductance which can indicate the ability of a material to conduct electricity. The conductance value can be used to calculate the

electrical conductivity value of the sample using the equation (2).

$$\sigma = \frac{Gd}{A} \tag{2}$$

where  $\sigma$  was the electrical conductivity ( $S \cdot cm^{-1}$ ),  $G$  was the conductance (S),  $d$  was the distance between the plates (cm), and  $A$  was the surface area ( $cm^2$ ).

While the activation energy for each hydrothermal temperature could be calculated from electrical conductivity analysis through equation (3).

$$\ln \sigma T = \ln \sigma_0 - \frac{E_a}{k} \frac{1}{T} \tag{3}$$

where  $\sigma$  was the electrical conductivity ( $S \cdot cm^{-1}$ ),  $\sigma_0$  is the constant ( $S \cdot cm^{-1}$ ),  $T$  is the temperature (K),  $E_a$  is the activation energy (eV), and  $k$  is the Boltzmann constant ( $8.617 \times 10^{-5} \text{ eV} \cdot K^{-1}$ ). The value of  $E_a/k$  is the slope in the obtained equation.

### 3. Results and Discussion

#### 3.1 Crystal phase and size of nano-silica

The structure of the rice husk nano-silica sample was analyzed at an  $2\theta$  angle of  $5^\circ$  to  $90^\circ$  as shown in Fig. 2. Fig. 2 shows that nano-silicas at 150, 200, and 250 °C have similar structure pattern, and have the highest diffraction peaks at  $2\theta$  of  $22.97^\circ$ ,  $23.06^\circ$ , and  $22.87^\circ$ , respectively. Based on the figure, it can be seen that the nano-silica produced in this study has the strongest peak at  $2\theta$  of  $22^\circ$  to  $23^\circ$ , which indicates that they are an amorphous phase of silicon dioxide (Irzaman et al., 2020). According to Yusof et al., (2010) in his research showed that the silica contained in rice husk ash had an amorphous phase with the strongest peak at  $2\theta$  of  $23^\circ$ .

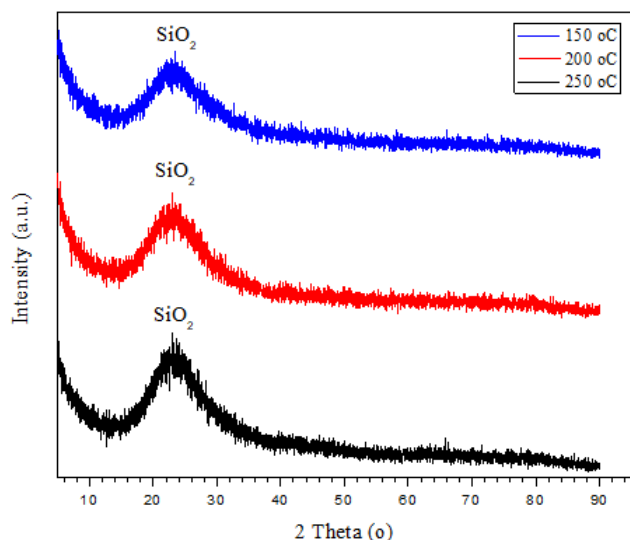


Fig. 2. Diffractogram of nano-silica at hydrothermal process temperature of 150 °C, 200 °C, and 250 °C

Table 1  
Crystal size and lattice strain of nano-silica

Hydrothermal temperature (°C)	Crystal size (nm)	Lattice strain
150	12.95	0.76
200	15.2	$4 \times 10^{-3}$
250	8.06	1.71

The crystal size was calculated using the Scherrer equation. Full Width at Half Maximum (FWHM) analysis means that the width of the diffraction peak at half the peak height is carried out using the Match! 3 software. Other factors that influence the magnitude of the FWHM value are the instrument factor and the lattice strain factor. Crystal size and lattice strain of nano-silica as shown in Table 1 were calculated using the curve between  $\beta \cos\theta$  to  $4\sin\theta$  so that a linear regression line was obtained for all compositions (Nasir et al., 2020).

Table 1 shows the effect of hydrothermal temperature on crystal size and lattice strain of the sample. Increasing the reaction temperature from 150 °C to 200 °C increases the crystal size. This can happen because the increase in temperature will accelerate crystal growth which involves the condensation process. In addition, the solubility can affect the crystal size. At low solubility, the ionic mobility becomes low and tends to cause the crystal size to become larger due to the crystallization process (Byrappa and Masahiro, 2001). However, the crystal size decrease again when the reaction temperature increased from 200 °C to 250 °C. This is because there is a rapid formation of several small crystals at higher temperatures due to the higher ionic mobility at high solubility, which competes for available chemical nutrients that do not occur at lower temperatures when the nucleation process occurs. High temperatures encourage nucleation more than crystal growth. The higher the hydrothermal temperature, the more crystal nuclei are formed so that the crystal growth takes longer, resulting in smaller crystal sizes (Maesaroh, 2020).

The FWHM value influences the crystal size, which a large FWHM value will cause a decrease in the value of the crystal size. The smaller the crystal size causes lead to the higher the lattice strain. The lattice strain value can interpret how much strain the atoms making up the compound have (Purwamargapratala and Purnama, 2010). The lattice strain value increases because the decrease in the crystal size will cause the distance between the atomic planes to become larger and make the lattice more stretched so that the lattice strain value increases (Qin and Szpunar, 2005).

#### 3.2 Particle size and distribution of nano-silica

Particle size results from the agglomeration process of primary particles so that one particle consists of more than one crystal (Setiawan, 2015). There are three types of distribution based on particle analysis data, namely intensity, volume, and amount. The particle size of the nano-silica that was successfully synthesized from rice husk is smaller than the size of the silica that has not been hydrothermally synthesized, and its size varies depending on the temperature variation of the hydrothermal process. The measurements using PSA can be seen in Table 2 with particle sizes in nanometers based on intensity distribution.

Table 2 shows the nano-silica of 150 °C, 200 °C, and 250 °C have average sizes of 1.95 nm, 0.54 nm, and 0.86 nm, respectively. Silica without hydrothermal treatment has average size of 864.26 nm. This indicates that the synthesized nano-silica from rice husks is successfully done by processing it in hydrothermal condition for 4 hours. While silica without hydrothermal treatment still do not reach nano scale particle category. Khan et al., (2019) reported that a material will belong to the nanoscale particle when it has a size of about 1-100 nm.

**Table 2**  
Particle size of nano-silica from rice husk ash

Hydrothermal treatment (°C)	Size (nm)	Average	Polydispersity index (PDI)
		size (nm)	
150	0.43-13.49	1.95	0.594
200	0.16-1.86	0.54	0.195
250	0.20-3.89	0.86	0.266

Increasing the temperature from 150 to 200 °C causes the particle size of nano-silica tend to decrease. However, by increasing the temperature from 200 to 250 °C, there is an increase in particle size. When the temperature increases, the solubility will increase, but when the temperature is increased again, the silica solubility tends to decrease (Setiawan, 2015). According to Byrappa and Masahiro (2001), high solubility conditions would result in high ionic mobility, low viscosity, and high ion concentration which will cause the agglomerate to separate then produce smaller particle sizes. However, when the temperature was increased again, the particle size increased again with better crystallinity (Mohammadikish, 2014). Based on the particle size analysis, it can be said that the untreated sample has a larger particle size than the synthesized nano-silica using hydrothermal.

Particle size distribution is related to polydispersity which is usually expressed in PDI (Polydispersity Index). The PDI shows the non-uniformity of the particle size. Yuan *et al.* (2010) stated that the smaller the PDI value, the more homogeneous the particle size. Avadi *et al.* (2010) also stated that the PDI which more than 0.5 indicates a high heterogeneity and it indicates a uniform particle size if the PDI value is close to 0. According to Nidhin *et al.* (2008), nanoparticles with an extensive size distribution will have a PDI more than 0.7. Meanwhile, Kafshgari *et al.* (2010) stated that a homogeneous dispersion has a PDI value close to zero, while a PDI value greater than 0.3 indicates a heterogeneous dispersion.

The increase in temperature from 150 °C to 200 °C also causes the PDI value to decrease with the PDI value at 200 °C process temperature of 0.195. This shows that the higher the hydrothermal temperature used, the smaller the PDI value will be. Likewise, Setiawan (2015) stated that the higher hydrothermal temperature would cause the PDI value to decrease. However, when the process temperature increases to 250 °C, the PDI value will increase to 0.266. According to Utomo (2015), the PDI value is influenced by the particle size range. The wider the range of particle sizes, the higher the PDI value will be. This causes the PDI value of nano-silica at 250 °C to be greater than the PDI of 200 °C. This is also due to the agglomeration process, which combines the primary particles with other primary particles to form secondary particles. In addition to increasing particle size, agglomeration will also increase the particle size non-uniformity (Utomo, 2015). Based on the three treatment temperatures of the hydrothermal process, it can be said that the size of the nano-silica obtained is more uniform with increasing treatment temperature, although, in this study, the smallest PDI was obtained at 200 °C.

### 3.3 Electrical conductivity analysis

This study collected data at 200 points with a frequency range of 50 Hz to 5 MHz to represent low to high frequencies. Thus, low, medium, and high frequencies are in the range of 50 Hz – 1000 Hz, 100 kHz – 500 kHz range, and 1 MHz – 5 MHz, respectively, which can be seen in Table 3.

Based on the value of electrical conductivity, a material can be grouped into conductors, semiconductors, and insulators. Conductor materials have electrical conductivity values in the range of  $10^{-3}$  to  $10^8$  S.  $\text{cm}^{-1}$ , semiconductor materials have electrical conductivity values in the range  $10^{-8}$  to  $10^{-3}$  S.  $\text{cm}^{-1}$ , and insulator materials have electrical conductivity values at a range from  $10^{-18}$  to  $10^{-8}$  S.  $\text{cm}^{-1}$  (Kwok, 1995). Table 4 shows that the synthesized nano-silica with various process temperatures of 150, 200, and 250 °C tends towards electrical conductivity values at low frequencies below  $10^{-8}$  S.  $\text{cm}^{-1}$ . This indicates that nano-silica of rice husk has insulating properties at low frequencies. Table 4 also shows that the nano-silica at all temperatures at medium and high frequencies are in the range of  $10^{-8}$  to  $10^{-3}$  S.  $\text{cm}^{-1}$ . This suggests that nano-silica at medium and high frequencies has semiconductor properties. Based on the electrical conductivity values at the three hydrothermal processing temperatures, it can be said that the produced nano-silicas have semiconductor properties with increasing frequency and process temperature, although the electrical conductivity value is very low. In addition to the increasing kinetic energy of the atoms, this is also because, at low frequencies, the impurity atoms have not yet vibrated, so they are insulators. Meanwhile, when the frequency increases, it causes the impurity atoms to vibrate, thereby increasing the electrical conductivity of the three samples (Har *et al.*, 2020).

Increasing the temperature from 150 to 200 °C causes higher electrical conductivity. This increase in temperature allows the vibration of atoms in the lattice to accelerate. However, by increasing the temperature from 200 to 250 °C, there is a decrease in electrical conductivity. The results of XRD characterization support this. The increase in electrical conductivity can be attributed to the increase in crystal size. The larger the crystal size, the closer the distance between the grains, so the potential for barriers between the grains is getting smaller. This causes the electron transfer process to be faster (Qin and Szpunar, 2005). In addition, to increase the electrical conductivity of nano-silica, energy is needed to activate the mobility of ions through the defects of the crystal structure. This energy is called the activation energy. The equation in Table 3 can determine the activation energy value for each hydrothermal temperature through equation (3). The equation is derived from electrical conductivity of nano-silicas, which can be seen in Fig. 3. Based on equation (3), the value of the activation energy of nano-silica at temperatures of 150, 200, and 250 °C are  $1.733 \times 10^{-6}$ ,  $2.207 \times 10^{-6}$ , and  $1.943 \times 10^{-6}$  eV, respectively. Increasing the temperature from 150 °C to 200 °C increases activation energy from  $1.7 \times 10^{-6}$  eV to  $2.2 \times 10^{-6}$  eV. However, the activation energy decreased at 250 °C to  $1.9 \times 10^{-6}$  eV. This shows that the higher the given temperature, the more the mobility of electrons moving from one grain to another so that the electrical conductivity is higher (Budiana, 2016).

**Table 3**  
The electrical conductivity of nano-silica at low, medium, and high frequencies

Frequency	Electrical conductivity ( $\times 10^{-7}$ S. $\text{cm}^{-1}$ )		
	150 °C	200 °C	250 °C
50 Hz - 1000 Hz (low)	0.018-2.1	0.014-2.63	0.0053-3.04
100 kHz - 500 kHz (medium)	0.34-12.3	0.209-13.17	0.234-9.6
1 MHz - 5 MHz (high)	0.39-164.2	4.48-184	4.48-165.9
Equation	$y = 7.597-0.0201x$	$y = 7.399-0.0256x$	$y = 7.396-0.0224x$

Note: the equation in Table related to Equation (3), where  $y$  is  $\ln \sigma T$ ; constant is  $\ln \sigma_0$ ; and  $x$  is  $\frac{1}{T}$

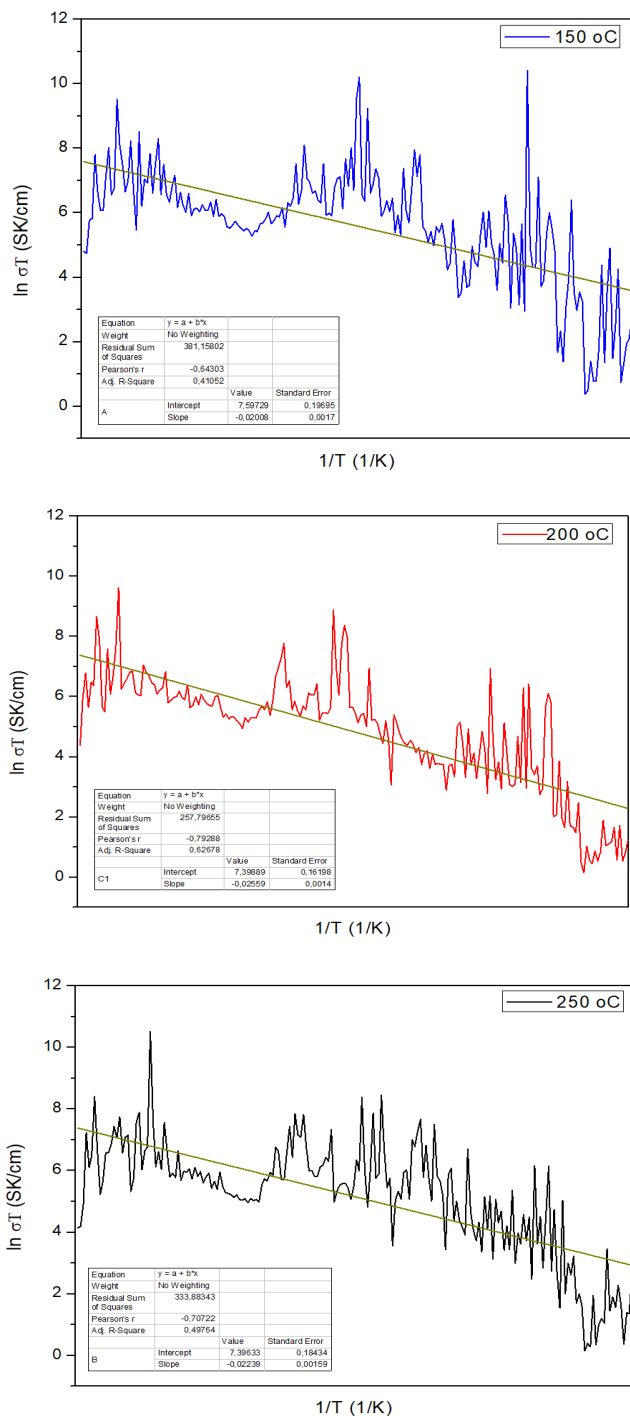


**Fig. 3.** Relationship of  $\ln \sigma T$  and  $1/T$  on nano-silicas at hydrothermal temperatures of 150, 200, and 250 °C

Based on this property, nano-silica of rice husk ash can be applied as semiconductor material for electronic industry. Suwanprateeb & Hatthapanit (2002) reported that rice-husk-ash-based silica was utilized as a filler for embedding composites in electronic devices. Another study such as Terada *et al.* (2022) converted recycled rice husk into orange-red Si Quantum Dot. In addition, it was found that the hydrothermal treatment of 200 °C for 4 hours and pressure of 2 atm is the optimum treatment in the manufacture of nanoparticles made from rice husk ash.

**6. Conclusion**

The synthesized nano-silica from rice husk has an amorphous phase with the highest diffraction angle at 2θ of 22° to 23°. Increasing the temperature would decrease the crystal size with the smallest crystal size of 8.06 nm and increase the lattice strain with the largest value of 1.71 at a temperature of 250 °C. The increase in temperature also decreases the particle size, with the smallest particle size of 0.813 nm at 200 °C. The particle size distribution of the synthesized nano-silicas at 200 °C and 250 °C were more homogeneous than nano-silica at 150 °C. The three variations of hydrothermal temperature indicate that the synthesized nano-silica was semiconducting at medium and high frequencies. In addition, the hydrothermal temperature of 200 °C was the optimum temperature for the manufacture of nano-silica from rice husks.

**Acknowledgements**

This research was funded by Hibah Penelitian Terapan Unggulan Perguruan Tinggi (PTUPT) from Deputy of Research and Development, Ministry of Research and Technology/National Research and Innovation Agency of Republic Indonesia with contract number: 1/E1/KP.PTNBH/2021.

**Author Contributions:** Irzaman: Conceptualization, project administration, methodology, formal analysis, Irmansyah: supervision, resources, Siti Aisyah: writing—original draft, project administration, Nazopatul Patonah Har: writing—review and editing, validation, Aminullah: writing—original draft, writing—review and editing,. All authors have read and agreed to the published version of the manuscript.

**Funding:** This research was funded by Hibah Penelitian Terapan Unggulan Perguruan Tinggi (PTUPT) from Deputy of Research and Development, Ministry of Research and Technology/National

Research and Innovation Agency of Republic Indonesia with contract number: 1/E1/KP.PTNBH/2021.

**Conflicts of Interest:** The authors declare no conflict of interest.

## References

- Adli, M. Z., Sari, M. Y., & Irzaman. (2018). Extraction silicon dioxide (SiO<sub>2</sub>) from charcoal of baggase (Saccharum officinarum L). *Earth and Environmental Science*, 187, 1-6. DOI: <https://doi.org/10.1088/1755-1315/187/1/012004>
- Aminullah, Rohaeti E, Yuliarto, & Irzaman. (2018). Reduction of silicon dioxide from bamboo leaves and its analysis using energy dispersive x-ray and fourier transform-infrared. *Earth and Environmental Science*, 209, 1-8. DOI: <https://doi.org/10.1088/1755-1315/209/1/012048>
- Avadi, M. R., Sadeghi, A. M. M, Mohammadpour, N., Abedin, S., Atyabi, F., Dinarvand, R., & Rafiee, T. M. (2010). Preparation and characterization of insulin nanoparticles using chitosan and Arabic gum with ionic gelation method. *Nanomedicine : nanotechnology, biology, and medicine*, 6(1), 58 - 53. DOI: <https://doi.org/10.1016/j.nano.2009.04.007>
- [BPS] Badan Pusat Statistik. (2019). *Luas Panen, Produksi, dan Produktivitas Padi Menurut Provinsi, 2018-2019*. Badan Pusat Statistik, Jakarta. In Indonesian
- Budiana. (2016). *Preparasi Elektrolit SOFC 8YSZ, 20 YBDC dan Pengaruh Co-firing Bi2O<sub>3</sub>-20 YBDC pada Sifat Listrik*. Thesis. Sepuluh Nopember Institute of Technology, Surabaya. In Indonesian
- Burkowicz, A., Galos, K., & Guzik, K. (2020). The resource base of silica glass sand versus glass industry development: The case of Poland. *Resources*, 9(11), 134. <https://doi.org/10.3390/resources9110134>
- Byrappa, K., & Masahiro, Y. (2001). *Handbook of Hydrothermal Technology*. Noyes Publications, New Jersey.
- Deviani, S. S, Mahatmanti, F. W., & Widiarti, N. (2018). Sintesis dan karakterisasi zeolit dari abu sekam padi menggunakan metode hidrotermal. *Indonesian Journal of Chemical Science*, 7(1), 87 - 93. DOI: 10.15294/IJCS.V7I1.24343
- Har, N. P., Palupi, Irmansyah, & Irzaman. (2020). Analysis of the electrical impedance and functional group of silicon dioxide (SiO<sub>2</sub>) from rice straw. *Earth and Environmental Science*, 460, 1-6. DOI: 10.1088/1755-1315/460/1/012031
- Hasri, H., Muharram, M., & Nadwo, F. (2020). A Synthesis nanosilica of bamboo's leaf (Bambusa Sp.) by using hydrothermal method. *Jurnal Kartika Kimia*, 3(2), 96-100. In Indonesian. DOI: <https://doi.org/10.26874/jkk.v3i2.56>
- Hossain, S. K. S., Mathur, L., & Roy, P. K. (2018). Rice husk/rice husk ash as an alternative source of silica in ceramics: A review. *Journal of Asian Ceramic Societies*, 6(4), 299-313. DOI: <https://doi.org/10.1080/21870764.2018.1539210>
- Husain, A. A. F., Hasana, W. Z. W., Shafie, S., Hamidon, M. N., & Pandey, S.S. (2018). A review of transparent solar photovoltaic technologies. *Renewable and Sustainable Energy Reviews*, 9, 779-791. DOI: <https://doi.org/10.1016/j.rser.2018.06.031>
- Iftitahiyah, V. N., Prasetyoko, D., Nur, H., Bahruji, H., & Hartati. (2018). Synthesis and characterization of zeolite NaX from Bangka Belitung Kaolin as alternative precursor. *Malaysian Journal of Fundamental and Applied Sciences*, 14(4), 414-418. DOI: 10.11113/mjfas.v14n4.964
- Irzaman, Cahyani, L. D., Aminullah, Maddu, A., Yuliarto, B., & Siregar U.J. (2020). Biosilica properties from rice huck using various HCl concentrations and frequencies sources. *Egyptian Journal of Chemistry*, 63(2), 363-371. DOI: 10.21608/EJCHEM.2019.8044.1679
- Irzaman, Oktaviani, & Irmansyah. (2018). Ampel bamboo leaves silicon dioxide (SiO<sub>2</sub>) extraction. *Earth and Environmental Science*, 141, 1-8. DOI: <https://doi.org/10.1088/1755-1315/141/1/012014>
- Irzaman, Yustaeni, D., Aminullah, Irmansyah, & Yuliarto, B. (2021). Purity, morphological, and electrical characterization of silicon dioxide from cogon grass (*Imperata cylindrica*) using different ashing temperatures. *Egyptian Journal of Chemistry*, 64(8), 4143-4149. DOI: 10.21608/EJCHEM.2019.15430.1962
- Jal, P. K., Sudarshan, M., Saha, A., Patel, S., & Mishra, B. K. (2004). Synthesis and characterization of nanosilica prepared by precipitation method. *Colloids and Surfaces A: Physicochemical and Engineering Aspects*, 240(1-3), 173–178. DOI: <https://doi.org/10.1016/j.colsurfa.2004.03.021>
- Kafshgari, M. H, Mohammad, K., Mobina, K., & Sahar, K. (2010). Reinforcement of chitosan nanoparticles obtained by an ionic cross-linking process. *Iranian Polymer Journal*, 20(5), 445-456.
- Khan, I., Saeed, K., & Khan, I. (2019). Nanoparticles: Properties, applications and toxicities. *Arabian Journal of Chemistry*, 12(7), 908-931. DOI: <https://doi.org/10.1016/j.arabjc.2017.05.011>
- Kwok, K. N. (1995). *Complete Guide to Semiconductor Device*. McGraw-Hill,inc., United States of America.
- Maesaroh. (2020). *Sintesis Nanosilika dari Daun Bambu Apus (Gigantaochlo apus) dengan variasi Suhu Proses Hidrotermal*. Thesis. IPB University, Bogor. In Indonesian
- Mohammadikish, M. (2014). Hydrothermal synthesis, characterization and optical properties of ellipsoid shape α-Fe<sub>2</sub>O<sub>3</sub> nanocrystals. *Ceramics Internasional*, 40, 1351-1358. DOI: 10.1016/j.ceramint.2013.07.016
- Nabeshi, H., Yoshikawa, T., Arimori, A., Yoshida, T., Tochigi, S., Hirai, T., Akase, T., Nagano, K., Abe, Y., Kamada, H., Tsunoda, Shinichi, Itoh, N., Yoshioka, Y., & Tsutsumi, Y. (2011). Effect of surface properties of silica nanoparticles on their cytotoxicity and cellular distribution in murine macrophages. *Nanoscale Research Letters*, 6 (23), 100-103. DOI: 10.1186/1556-276X-6-93
- Nasir, H., Rahman, N., Zulfiqar, Khan, T, Ali, S., Khan, R., & Hayat, K. (2020). Variations in structural, optical, and dielectric properties of CuO nanostructures with thermal decomposition. *Journal of Materials Science: Materials in Electronics*, 31(13), 1-8. DOI: 10.1007/s10854-020-03614-1
- Nidhin, M., Indumathy, R., Sreeram, K. J., and Nair, B. U. (2008). Synthesis of iron oxide nanoparticles of narrow size distribution on polysaccharide templates. *Bulletin of Materials Science*, 31(1), 93-96. DOI: 10.1007/s12034-008-0016-2
- Nikmatin, S., Purwanto, S., Maddu, A., Mandang, T., & Purwanto, A. (2012). Analisis struktur selulosa kulit rotan dengan filler bionanokomposit dengan difraksi sinar-X. *Jurnal Sains Materi Indonesia*, 13(2), 97-102. In Indonesian. DOI: 10.17146/jsmi.2012.13.2.4712
- Purwamargapratala, Y., & Purnama, S. (2010). Regangan kisi dan ukuran butir elektrolit padat komposit alkali-alumina. *Urania*, 16(2), 98-104. In Indonesian. DOI: <http://dx.doi.org/10.17146/urania.2010.16.2.2434>
- Qin, W. & Szpunar, J. A. (2005). Origin of lattice strain in nanocrystalline materials. *Philosophical Magazine Letters*, 85(12), 649-656. DOI: <https://doi.org/10.1080/09500830500474339>
- Rahma, C. (2017). Sintesis dan karakterisasi material fotokatalis Na<sub>2</sub>Ti<sub>6</sub>O<sub>13</sub> menggunakan metode hidrotermal. *Jurnal Optimalisasi*, 3(4), 28-38. In Indonesian. DOI: <https://doi.org/10.35308/jopt.v3i4.263>
- Rahman, I. A., & Padavettan, V. (2012). Synthesis of silica nanoparticles by sol-gel: Size-dependent properties, surface modification, and applications in silica-polymer nanocomposites—a review. *Journal of Nanomaterials*, 2012, 1-5. DOI: <https://doi.org/10.1155/2012/132424>
- Rohaeti, E., Hikmawati, & Irzaman. (2010). Production of semiconductor materials silicon from silica rice husk waste as alternative silicon. *Materials Science and Technology*, 265 - 272.
- Setiawan, W. K. (2015). *Preparasi Nanosilika dari Abu Ketel dengan Metode Kopresipitasi sebagai Aditif Membran Elektrolit Berbasis Kitosan*. Thesis. IPB University, Bogor. In Indonesian
- Suwanprateeb, J. & Hatthapanit, K. (2002). Rice-husk-ash-based silica as a filler for embedding composites in electronic devices. *Journal of Applied Polymer Science*, 86, 3013-3020. DOI: 10.1002/app.11291

- Terada, S., Ueda, H., Ono, T., & Saitow, K. -I. (2022). Orange-red Si quantum dot LEDs from recycled rice husks. *ACS Sustainable Chemistry & Engineering*, 10(5), 1765-1776. DOI: <https://doi.org/10.1021/acssuschemeng.1c04985>
- Toshtay, K. & Auezov, A. B. (2020). Hydrogenation of vegetable oils over a palladium catalyst supported on activated diatomite. *Catalysis in Industry*, 12(1), 7-15. DOI: 10.1134/S2070050420010109
- Utomo, S.S. (2015). *Sintesis dan Pencirian Nanosilika Berbahan Dasar Abu Ketel Industri Gula dengan Variasi Waktu Aging dan pH Presipitasi*. Thesis. IPB University, Bogor. In Indonesian
- Verina, H. (2014). *Optimasi Kelajuan Suhu Annealing untuk Ekstraksi Silika dari Abu Sekam Padi serta Uji Kandungan Molekul*. Thesis. IPB University, Bogor. In Indonesian
- Yazdani, A., Rezaie, H. R., & Ghassai, H. (2010). Investigation of hydrothermal synthesis of wollastonite using silica and nano silica at different pressures. *Journal of Ceramic Processing Research*. 11(3), 348~353. DOI: 10.36410/jcpr.2010.11.3.348
- Yuan, H., Gao, F., Zhang, Z., Miao, L., Yu, R., Zhao, H., & Lan, M. (2010). Study of controllable preparation of silica nanoparticles with multi-sized and their size-dependent cytotoxicity in pheochromocytoma cells and human embryonic kidney cells. *Journal of Health Science*, 56 (6), 632-640. DOI: 10.1248/jhs.56.632
- Yusof, A. M, Nizam, N. A, & Rashid, N. A. (2010). Hydrothermal conversion of rice husk ash to faujasite-types and NaA-type of zeolite. *Journal of Porous Mater*, 17(1), 39-47. DOI: 10.1007/s10934-009-9262-y
- Yuvakkumar, R., Elango, V., Rajendran, V., & Kannan, N. (2012). High-purity nanosilica powder from rice husk using a simple chemical method. *Journal of Experiment Nanoscience*, 9(3), 272-281. DOI: <https://doi.org/10.1080/17458080.2012.656709>



© 2022. The Authors. This article is an open access article distributed under the terms and conditions of the Creative Commons Attribution-ShareAlike 4.0 (CC BY-SA) International License (<http://creativecommons.org/licenses/by-sa/4.0/>)